Original papers
Nanostructured, nanoscale materials and nanodevices

УДК 543.424 DOI: 10.17277/jamt-2025-10-04-313-320

A study of the structure of carbon nanomaterials by Raman spectroscopy: analysis of spectra of commercial samples of graphite, nanotubes and carbon blacks

© Elena V. Kuzmina[a]✉, Elvina R. Gaifullina [a,b], Alena M. Ionina[a], Elena V. Karaseva[a], Vladimir S. Kolosnitsyn[a]

[a] *Ufa Institute of Chemistry of Ufa Federal Research Centre of the Russian Academy of Sciences, 69, Oktyabrya Av., Ufa, 450054, Russian Federation,*
[b] *Akmulla Bashkir State Pedagogical University, 3a, Oktyabrskoy Revolyutsii St., Ufa, 450077, Russian Federation*

✉ kuzmina@anrb.ru

Abstract: This paper summarizes the results of structural investigations of carbon nanomaterials using Raman spectroscopy. The conducted research revealed that the distances between defects are 26–43 nm in graphites, 12–16 nm in multi-walled carbon nanotubes (MWCNTs) and 11–15 nm in carbon black. It is shown that the Raman spectra of high-quality graphites and graphenes are characterized by a narrow G band (width less than 35 cm^{-1}), intensity ratio $I_{(D)}/I_{(G)} < 0.3$. The Raman spectra of carbon nanotubes are characterized by wide G bands (width > 50 cm^{-1}), high $I_{(D)}/I_{(G)}$ ratio (> 0.5) and the presence of 2D bands with a maximum position of about 2670 cm^{-1}. The Raman spectra of carbon blacks are characterized by a strongly broadened G band (width > 70 cm^{-1}), the $I_{(D)}/I_{(G)}$ ratio is close to 1 and more. The presence, position and width of 2D bands are sensitive to the structures of carbon materials. For ordered graphites, the position of the 2D band maximum is about 2680 cm^{-1}, and their width is < 85 cm^{-1}. For MWCNTs, the 2D band maximum is in the range of 2670–2690 cm^{-1}, and the band width is about 90–100 cm^{-1}. In the Raman spectra of carbon blacks, the 2D band may be absent; the position of the maximum may be shifted to the long-wave or short-wave regions, the 2D band is strongly broadened (width > 150 cm^{-1}).

Keywords: Raman spectroscopy; graphite; carbon nanotubes; carbon black.

For citation: Kuzmina EV, Gaifullina ER, Ionina AM, Karaseva EV, Kolosnitsyn VS. A study of the structure of carbon nanomaterials by Raman spectroscopy: analysis of spectra of commercial samples of graphite, nanotubes and carbon blacks. *Journal of Advanced Materials and Technologies*. 2025;10(4):313-320. DOI: 10.17277/jamt-2025-10-04-313-320

Исследование структуры углеродных наноматериалов методом спектроскопии комбинационного рассеяния: анализ спектров коммерческих образцов графитов, нанотрубок и саж

© Е. В. Кузьмина[a]✉, Э. Р. Гайфуллина [a,b], А. М. Ионина [a], Е. В. Карасева [a], В. С. Колосницын [a]

[a] *Уфимский Институт химии Уфимского федерального исследовательского центра Российской академии наук, пр. Октября, 69, Уфа, 450054, Российская Федерация,*
[b] *Башкирский государственный педагогический университет им. М. Акмуллы, ул. Октябрьской революции, 3а, Уфа, 450077, Российская Федерация*

✉ kuzmina@anrb.ru

Аннотация: В статье суммированы результаты исследований структуры углеродных наноматериалов методом спектроскопии комбинационного рассеяния (КР). В результате проведенных исследований установлено, что расстояния между дефектами в графитах находятся в диапазоне 26…43 нм, углеродных многостенных углеродных

нанотрубок (МУНТ) – 12…16 нм и саж 11…15 нм. Показано, что для КР-спектров высококачественных графитов и графенов характерны узкая G-полоса (ширина менее < 35 см$^{-1}$), соотношение интенсивностей $I_{(D)}/I_{(G)}$) < 0,3. Для КР-спектров углеродных нанотрубок характерны широкие G-полосы (ширина > 50 см$^{-1}$), высокое соотношение $I_{(D)}/I_{(G)}$ (> 0,5) и наличие 2D-полос с положением максимума около 2670 см$^{-1}$. Для КР-спектров саж характерно сильно уширенная G-полоса (ширина > 70 см$^{-1}$), соотношение $I_{(D)}/I_{(G)}$ близко к 1 и более. Наличие, положение и ширина 2D-полос чувствительны к структурам углеродных материалов. Для упорядоченных графитов положение максимума 2D-полос составляет порядка 2680 см$^{-1}$, а их ширина менее < 85 см$^{-1}$. Для МУНТ максимум 2D-полосы находится в диапазоне 2670…2690 см$^{-1}$, а ширина полосы порядка 90…100 см$^{-1}$. На КР-спектрах саж 2D-полоса может отсутствовать; положение максимума может быть смещено в длинноволновую или коротковолновую области, 2D-полоса сильно уширена (ширина > 150 см$^{-1}$).

Ключевые слова: спектроскопия комбинационного рассеяния; графит; углеродные нанотрубки; сажи.

Для цитирования: Kuzmina EV, Gaifullina ER, Ionina AM, Karaseva EV, Kolosnitsyn VS. A study of the structure of carbon nanomaterials by Raman spectroscopy: analysis of spectra of commercial samples of graphite, nanotubes and carbon blacks. *Journal of Advanced Materials and Technologies*. 2025;10(4):313-320. DOI: 10.17277/jamt-2025-10-04-313-320

1. Introduction

Carbon materials are widely used as components of electrodes in electrochemical energy storage devices such as supercapacitors, lithium-ion, and post-lithium-ion batteries. The properties of carbon materials strongly depend on their atomic structure, degree of ordering, type and concentration of defects, as well as the dimensional characteristics of their constituent elements [1–4].

Studying the structure of carbon nanomaterials is important for understanding their properties. Traditional analytical methods, such as electron microscopy and X-ray diffraction, provide valuable information about macrostructure and crystalline order [5–9]. However, these techniques do not fully describe the structure, degree of ordering, and defects of carbon materials. A comprehensive structural description of carbons requires the use of multiple complementary methods.

It is well known that Raman spectra (RS) of carbon materials are sensitive to the structure and allotropic form of carbon [9–11]. For this reason, Raman spectroscopy is widely applied to study the structural organization of carbons [12–20]. Raman spectra can provide information about the size of atomically ordered domains in carbon materials, their structure, type of mutual ordering, atomic geometry of boundaries, and many other important characteristics [9, 10, 21–28].

The shape of Raman spectra of carbons depends on several factors, including the presence of clusters of sp^2-hybridized carbon atoms, the degree of disorder, the presence of rings and chains composed of sp^2-hybridized carbon atoms, and the ratio of sp^2 to sp^3 hybridized carbon atoms [12, 29]. If the carbon material contains sp^2 carbon networks, the G band (~1580 cm^{-1}) appears in the Raman spectrum. In the presence of sp^3 and sp carbon networks, characteristic D (~1330 cm^{-1}, diamond) and D′ (1850–2100 cm^{-1}, linear chains of sp^2 carbon atoms) bands are observed [30]. Structurally ordered 3D graphites also exhibit a 2D (or G′) band in the 2500–2800 cm^{-1} region [30]. The 2D band corresponds to the second overtone of the D band [30].

The D band may show dispersion depending on the excitation energy [20]. However, the higher the degree of disorder, the smaller the D band dispersion – which is opposite to the behavior of the G band [29]. The full width at half maximum (hereafter referred to as the width) of the G band always increases with increasing disorder [31], while the position of the G band maximum shifts toward shorter wavelengths [19].

Broadening of the D band may indicate changes in the size of rings within graphene layers (with 5- and 7-membered rings appearing instead of 6-membered ones) [17].

In structurally disordered carbons, the maximum of the G band shifts toward the long-wavelength region as the excitation wavelength decreases (from the infrared to the ultraviolet range) [29]. The shift of the G band maximum position with changing laser wavelength depends on the degree of disorder in the carbon structure and on the configuration of the sp^2-hybridized carbon atoms.

Based on the shift of the G band maximum position with decreasing laser wavelength, carbons can be classified into two types:

Type 1. In materials containing only sp^2-hybridized rings, the G band shift does not exceed approximately 1600 cm^{-1}.

Type 2. In materials containing sp^2-hybridized chains (such as amorphous carbon and diamond-like carbon), the G band maximum shifts to the long-

wavelength region beyond 1600 cm^{-1} and may reach up to 1690 cm^{-1} when excited with radiation at a wavelength of 229 nm [29, 32, 33].

Thus, the position and shape of the bands in the Raman spectra of carbon materials can provide information about their structure. The G band characterizes the degree of disorder in the carbon material, and the relative intensity of the G peak increases with the number of graphene layers. The D band reflects the degree of structural disorder near the boundaries of microcrystalline regions, which reduces their symmetry.

The aim of this work was to study the microstructure of various commercial nanostructured allotropic forms of carbon materials using Raman spectroscopy.

2. Materials and Methods

2.1. Materials under study

The following carbon materials were used in this study:

(a) Graphites and graphene: Timrex® SLP50 (TIMCAL Graphite & Carbon); synthetic graphite (Dianshi); natural Korean graphite (NG-10); graphite (Alpha); multilayer graphene GLNP-0350 (GraphenLab).

(b) Carbon fibers and nanotubes: Nano fiber ENF 100AA-GFE (carbon nanofibers, Electrovac AG); Pyrograf II™ (carbon fiber HT grade, highly graphitic carbon nanofiber, Pyrograf Products, Inc.); MWCNT Graphistrength® U100 (Arkema); MWCNT Graphistrength® C100 (Arkema); MWCNT BAYTUBES® C70P (Bayer AG); MWCNT LUCANTM CP1001M (LG Chem); Taunit–MD (NanoTechCenter LLC).

(c) Carbon blacks: Ketjenblack® EC-600JD (Akzo Nobel Polymer Chemicals LLC); PRINTEX® XE2 (Degussa AG); Monarch® 1300 (Cabot Corp.); Monarch® 1400 (Cabot Corp.); Super P™ Li (TIMCAL Graphite & Carbon); activated carbon black Bau-MF.

2.2. Characterization methods

Raman spectra of the samples were obtained using an EnSpectr R532 Raman spectrometer equipped with a 532 nm laser operating at an optical power of 30 mW. The laser spot diameter was 0.6 μm. Spectra were recorded in the 150–6000 cm^{-1} range with a spectral resolution of 5–8 cm^{-1}.

The carbon materials were used without any preliminary treatment. Samples for Raman measurements were in powder form.

When processing the Raman spectra of the carbon materials, it was assumed that they belong to Stage 1 according to the classification proposed by Ferrari and Robertson**,** with an average interdefect distance L_D greater than 10 nm, which can be calculated using Equation (1) [9, 29, 32, 33]:

$$L_D^2 = \frac{4.3 \cdot 10^3}{E_L^4} \left[\frac{I_{(D)}}{I_{(G)}} \right]^{-1}, \quad (1)$$

where L_D is the average distance between defects (nm); E_L is the laser energy eV; $I_{(D)}$ and $I_{(G)}$ are the intensities of the D and G bands, respectively.

3. Results and Discussion

3.1. Raman spectra of graphites

In the Raman spectra of graphite samples (Fig. 1), three characteristic bands are observed: D, G, and 2D. The position of the G band maximum varies within the frequency range of 1563–1576 cm^{-1}, the D band within 1340–1342 cm^{-1}, and the 2D band within 2674–2690 cm^{-1}. All bands are relatively narrow and well defined. A weakly resolved D′ band can also be observed as a shoulder on the G band at 1620–1650 cm^{-1}. The intensity ratio $I_{(D)}/I_{(G)}$ does not exceed 0.2 (Table 1).

The relatively narrow width and position of the 2D band correspond to the structure of multilayer graphene or highly ordered graphite. The shape and position of the 2D band maximum confirm the predominance of sp^2 structures.

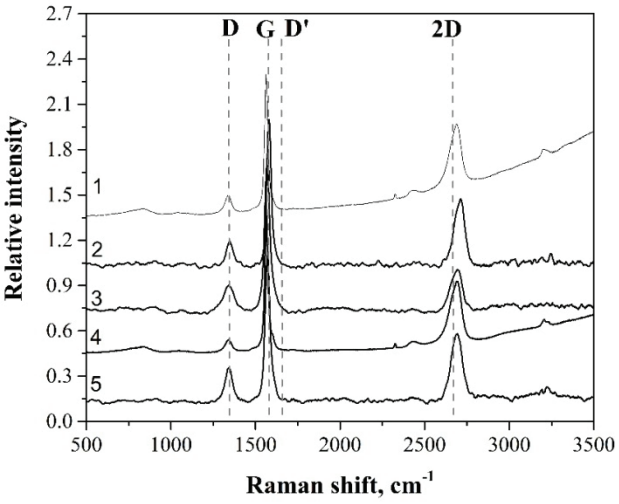

Fig. 1. Raman spectra of graphites and graphenes. Designations of carbon materials on the graph: *1* – Timrex SLP50; *2* – Alpha; *3* – NG-10; *4* – Graphene CLNP_0350; *5* – Dianshi

Table 1. Parameters of the microstructure of carbon materials calculated from Raman spectra

Samples	D band		G band		2D band		$\frac{I_{(D)}}{I_{(G)}}$	L_D, nm
	λ, cm^{-1}	FWHM, cm^{-1}	λ, cm^{-1}	FWHM, cm^{-1}	λ, cm^{-1}	FWHM, cm^{-1}		
Graphite and graphene								
Timrex SLP50	1339	45	1563	26	2683	77	0.13	34
Graphene GLNP-0350	1340	45	1564	26	2684	80	0.08	43
Dianshi	1342	50	1571	29	2690	78	0.22	26
Alpha	1341	89	1576	69	2674	83	0.14	32
NG-10	1342	75	1569	33	2687	81	0.16	30
Carbon nanotubes								
Taunit-MDTM	1341	68	1580	59	2693	89	0.56	16
Baytubes® C70P	1337	59	1573	69	2674	87	1.06	12
Graphistrength® U100	1335	71	1572	62	2670	94	1.03	12
Graphistrength® C100	1333	64	1569	70	2666	95	1.02	12
LUCAN TM CP1001M	1332	70	1569	77	2670	99	1.05	12
Carbon black								
PrintexXE2	1341	64	1576	73	2717	292	1.08	12
Super® Li	1338	81	1561	130	2541	356	0.69	15
Ketjenblack® EC-600JD	1329	85	1576	93	2655	174	1.11	11
Monarch 1300	1347	111	1572	149	n/a	n/a	0.77	14
Monarch 1400	1347	112	1575	133	n/a	n/a	0.69	15
BAU MF	1341	212	1562	147	n/a	n/a	1.03	12

The D band width is about 45 cm^{-1}, except for the NG-10 and Alpha samples, for which FWHM(D) values are 75 and 89 cm^{-1}, respectively. The G band width ranges from 26 to 30 cm^{-1}, except for the Alpha sample, which exhibits a width of 69 cm^{-1} (Table 1). The 2D band width for all graphite samples lies within 77–83 cm^{-1}.

It is worth noting that the Raman spectrum of the commercial graphene sample Graphene CLNP_0350 corresponds to that of well-ordered graphite.

3.2. Raman spectra of carbon nanotubes

The Raman spectra of MWCNTs exhibit D, D′, G, and 2D bands (Fig. 2). In addition to the main bands, broadened asymmetric bands are observed at approximately 850 and 1050 cm^{-1}, which are associated with defects, and a band at ~2950 cm^{-1} corresponding to a combination mode (D + G) induced by the presence of defects [30, 34].

The D band maxima of the carbon nanotubes are in the range 1332–1343 cm^{-1}, while the 2D band maxima are in the range 2666–2693 cm^{-1}. The G band maximum in the MWCNT spectra occurs within 1569–1586 cm^{-1}, which is characteristic for carbon nanotubes. The G band maximum of Taunit-MD™ (1580 cm^{-1}) is slightly shifted toward the long-wavelength region, likely due to the presence of amorphous carbon and/or the nanotube diameter. The positions of the G, D, and 2D bands are consistent with those expected for multi-walled carbon nanotubes.

The G bands are significantly broader than those of high-quality graphite or graphene (by a factor of 2–3). This is a typical feature of MWCNTs, attributed to their cylindrical geometry and the possible presence of defects or amorphous phases.

The intensity ratio $I_{(D)}/I_{(G)}$ is substantially higher than that of graphite or graphene (see Table 1). This is a distinguishing characteristic of MWCNTs

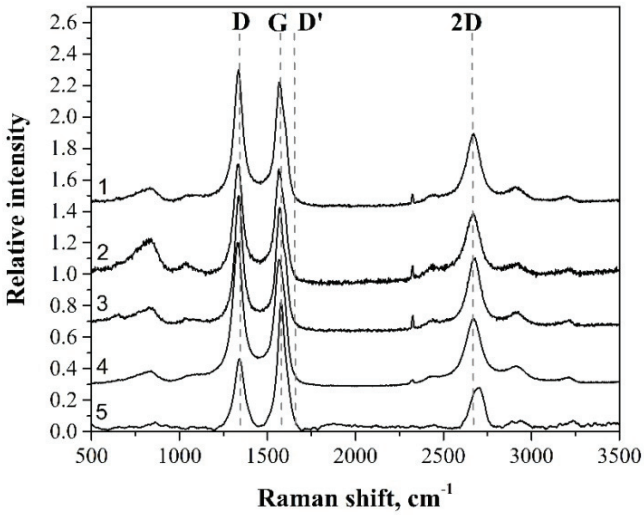

Fig. 2. Raman spectra of carbon nanotubes.
Designations of carbon materials on the graph:
1 – Graphistrength® U100; *2* – Graphistrength® C100;
3 – Baytubes® C70P; *4* – LUCAN TM CP1001M;
5 – TAUNIT-MD TM

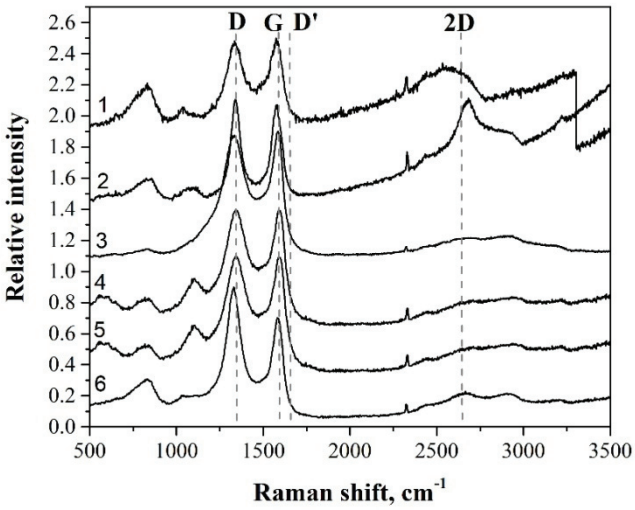

Fig. 3. Raman spectra of carbon blacks.
Designations of carbon materials on the chart:
1 – Super Li carbon black; *2* – PrintexXE2; *3* – Bau-MF;
4 – Monarch 1300; *5* – Monarch 1400;
6 – Ketjenblack® EC-600JD

and is related both to edge effects of the tubes and to the possible presence of defects or amorphous carbon. High values (1.02–1.06) for Graphistrength® and LUCAN™ CP1001M indicate either small nanotube diameters or a relatively high level of defects/impurities.

The calculated average interdefect distances L_D are significantly smaller than those of graphite (see Table 1), which is consistent with the nanoscale nature of MWCNTs and their characteristically high $I_{(D)}/I_{(G)}$ ratio.

3.3. Raman spectra of carbon blacks

The Raman spectra of carbon blacks are characterized by intense D and G bands, as well as a low-intensity, broad 2D band (Fig. 3). The D band maximum is located in the range of 1330–1347 cm^{-1}, while the G band maximum falls within 1560–1576 cm^{-1}. The 2D band is absent in the spectra of Monarch 1300, Monarch 1400, and Bau-MF carbon blacks.

Broadened asymmetric bands are also observed at approximately 850 and 1050 cm^{-1}, which are associated with defects. Notably, the relative intensity of these bands is higher than in carbon nanotubes, indicating a higher defect density in carbon blacks compared to nanotubes.

The G bands are significantly broadened, with widths ranging from 70 to 150 cm^{-1}. The intensity ratio $I_{(D)}/I_{(G)}$ is close to or exceeds 1, except for Super® Li and Monarch 1400. The 2D bands are also substantially broadened, with widths in the range of 170–360 cm^{-1}.

The calculated interdefect distances L_D are comparable to the crystallite sizes of MWCNTs and are significantly smaller than those of graphite (see Table 1).

The pronounced broadening of the G and 2D bands, the $I_{(D)}/I_{(G)}$ ratio close to unity, and the presence of bands at ~850 and 1050 cm^{-1} indicate high defect density and small crystallite size in these carbon blacks.

Thus, based on the analysis of the recorded Raman spectra of commercial carbon material samples, the following conclusions can be drawn:

– The Raman spectra of high-quality graphite and graphene are characterized by a narrow G band (width < 35 cm^{-1}) and an intensity ratio $I_{(D)}/I_{(G)} < 0.3$;

– The Raman spectra of carbon nanotubes are characterized by broad G bands (width > 50 cm^{-1}), a high $I_{(D)}/I_{(G)}$ ratio (> 0.5), and the presence of 2D bands with maxima around 2670 cm^{-1};

– The Raman spectra of carbon blacks exhibit a significantly broadened G band (width > 70 cm^{-1}), $I_{(D)}/I_{(G)}$ ratio close to or exceeding 1, and a 2D band that is either absent or strongly broadened (width > 150 cm^{-1}).

The presence, position, and width of the 2D bands are sensitive to the structure of the carbon materials.

In ordered graphites, the 2D band maximum is around 2680 cm^{-1}, and the width is less than 85 cm^{-1}.

In MWCNTs, the 2D band maximum lines in the range 2670–2690 cm^{-1}, with a width of approximately 90–100 cm^{-1}. In carbon blacks, the 2D band may be absent; its maximum can be shifted toward either the long- or short-wavelength region, and the band is strongly broadened (width > 150 cm^{-1}).

The $I_{(D)}/I_{(G)}$ ratio should only be compared for carbon materials of the same type. High values in graphite/graphene ($I_{(D)}/I_{(G)} > 0.2$) indicate the presence of defects, whereas for carbon nanotubes and carbon blacks, $I_{(D)}/I_{(G)}$ values of 0.5–1.0 are typical.

4. Conclusion

The Raman spectra of various carbon forms – graphite, nanotubes, and carbon blacks – were analyzed.

It was found that the average interdefect distances are:

– 26–43 nm for graphite;

– 12–16 nm for multi-walled carbon nanotubes;

– 11–15 nm for carbon blacks.

Carbon nanofibers and nanotubes occupy an intermediate position in terms of grain size and interdefect distance, having a less ordered structure compared to graphite but more ordered than carbon blacks.

Thus, analysis of the D, G, and 2D band parameters (position, width, intensity ratio) allows reliable classification of materials, assessment of structural perfection, crystallinity, and defect density, and comparative evaluation of commercial products. The G band width and 2D band characteristics are particularly informative.

5. Funding

The work was carried out as part of the State Assignment on the topic of Research Work at the Ufa Institute of Chemistry, Ufa Scientific Center, Russian Academy of Sciences, No. 124032600061-3.

6. Conflict of interest

The authors declare no conflict of interest.

References

1. Geim AK, Novoselov KS. The rise of graphene. *Nature Materials*. 2007;6(3):183-191. DOI:10.1038/nmat1849

2. Islam MH, Afroj S, Uddin MA, Andreeva DV, et al. Graphene and CNT-based smart fiber-reinforced composites: a review. *Advanced Functional Materials*. 2022;32(40):2205723. DOI:10.1002/adfm.202205723

3. Wu X, Mu F, Zhao H. Recent progress in the synthesis of graphene/CNT composites and the energy-related applications. *Journal of Materials Science & Technology*. 2020;55:16-34. DOI:10.1016/j.jmst.2019.05.063

4. Labunov VA, Tabulina LV, Komissarov IV, Trapov DV, et al. Features of graphene reduction from graphene oxide. *Zhurnal Fizicheskoy Khimii = Russian Journal of Physical Chemistry A*. 2017;(6):1018-1023. DOI:10.7868/S0044453717060176 (In Russ.)

5. Kang DS, Lee SM, Lee SH, Roh JS. X-ray diffraction analysis of the crystallinity of phenolic resin-derived carbon as a function of the heating rate during the carbonization process. *Carbon Letters*. 2018;27:108-111. DOI:10.5714/CL.2018.27.108

6. Lee SM, Lee SH, Roh JS. Analysis of activation process of carbon black based on structural parameters obtained by XRD analysis. *Crystals*. 2021;11(2):153. DOI:10.3390/cryst11020153

7. Bessonov VB. Microfocus X-ray tubes. *Journal of the Russian Universities*. *Radioelectronics*. 2021;24(5):6-21. DOI:10.32603/1993-8985-2021-24-5-6-21

8. Tan WH, Lee SL, Chong CT. TEM and XRD analysis of carbon nanotubes synthesised from flame. *Key Engineering Materials*. 2016;723:470-475. DOI:10.4028/www.scientific.net/KEM.723.470

9. Ferrari AC, Basko DM. Raman spectroscopy as a versatile tool for studying the properties of graphene. *Nature Nanotechnology*. 2013;8(4):235-246. DOI:10.1038/nnano.2013.46

10. Li Z, Deng L, Kinloch IA, Young RJ. Raman spectroscopy of carbon materials and their composites: graphene, nanotubes and fibres. *Progress in Materials Science*. 2023;135:101089. DOI:10.1016/j.pmatsci.2023.101089

11. Ziatdinov AM. Raman spectroscopy of nanoscale honeycomb carbon structures. *Vestnik Dal'nevostochnogo Otdeleniya Rossiyskoy Akademii Nauk*. 2020;(6(214)):27-40. DOI:10.37102/08697698.2020.214.6.003 (In Russ.)

12. Verzhbitskiy IA, Corato MD, Ruini A, Molinari E, et al. Raman fingerprints of atomically precise graphene nanoribbons. *Nano Letters*. 2016;16(6):3442-3447. DOI:10.1021/acs.nanolett.5b04183

13. Zhang J, Perrin ML, Barba L, Overbeck J, et al. High-speed identification of suspended carbon nanotubes using Raman spectroscopy and deep learning. *Microsystems & Nanoengineering*. 2022;8(1):19. DOI:10.1038/s41378-022-00350-w

14. Finnie P, Ouyang J, Fagan JA. Static and dynamic Raman excitation mapping of chirality-pure carbon nanotube films. *Communications Materials*. 2025;6(1):10. DOI:10.1038/s43246-024-00727-6

15. Lucchese MM, Stavale F, Ferreira EHM, Vilani C, et al. Quantifying ion-induced defects and Raman relaxation length in graphene. *Carbon*. 2010;48(5):1592-1597. DOI:10.1016/j.carbon.2009.12.057

16. Cançado LG, Monken VP, Campos JLE, Santos JCC, et al. Science and metrology of defects in graphene using Raman spectroscopy. *Carbon*. 2024;220:118801. DOI:10.1016/j.carbon.2024.118801

17. Liu X, Choi J, Xu Z, Grey CP, et al. Raman spectroscopy measurements support disorder-driven capacitance in nanoporous carbons. *Journal of the American Chemical Society*. 2024;146(45):30748-30752. DOI:10.1021/jacs.4c10214

18. Senda T, Tanaka F, Ishikawa T, Okino S, et al. Developing a novel evaluation technique of Raman spectra for pan-based carbon fibers using dependence of excitation wavelength and differential spectra. *Carbon*. 2025;234:119970. DOI:10.1016/j.carbon.2024.119970

19. Yuan R, Guo Y, Gurgan I, Siddique N, et al. Raman spectroscopy analysis of disordered and amorphous carbon materials: a review of empirical correlations. *Carbon*. 2025;238:120214. DOI:10.1016/j.carbon.2025.120214

20. Madito MJ. Revisiting the Raman disorder band in graphene-based materials: a critical review. *Vibrational Spectroscopy*. 2025;139:103814. DOI:10.1016/j.vibspec.2025.103814

21. Ribeiro-Soares J, Oliveros ME, Garin C, David MV, et al. Structural analysis of polycrystalline graphene systems by Raman spectroscopy. *Carbon*. 2015;95:646-652. DOI:10.1016/j.carbon.2015.08.020

22. Jorio A, Souza Filho AG. Raman studies of carbon nanostructures. *Annual Review of Materials Research*. 2016;46(1):357-382. DOI:10.1146/annurev-matsci-070115-032140

23. Eckmann A, Felten A, Mishchenko A, Britnell L, et al. Probing the nature of defects in graphene by Raman spectroscopy. *Nano Letters*. 2012;12(8):3925-3930. DOI:10.1021/nl300901a

24. Mohan AN, Manoj B, Ramya AV. Probing the nature of defects of graphene like nano-carbon from amorphous materials by Raman spectroscopy. *Asian Journal of Chemistry*. 2016;28(7):1501-1504. DOI:10.14233/ajchem.2016.19739

25. Cançado LG, Takai K, Enoki T, Endo M, et al. Measuring the degree of stacking order in graphite by Raman spectroscopy. *Carbon*. 2008;46(2):272-275. DOI:10.1016/j.carbon.2007.11.015

26. Cançado LG, Pimenta MA, Neves BRA, Dantas MSS, et al. Influence of the atomic structure on the Raman spectra of graphite edges. *Physical Review Letters*. 2004;93(24):247401. DOI: 10.1103/PhysRevLett.93.247401

27. Cançado LG, Takai K, Enoki T, Endo M, et al. General equation for the determination of the crystallite size la of nanographite by Raman spectroscopy. *Applied Physics Letters*. 2006;88(16):163106. DOI:10.1063/1.2196057

28. Bokobza L, Bruneel JL, Couzi M. Raman spectroscopy as a tool for the analysis of carbon-based materials (highly oriented pyrolitic graphite, multilayer graphene and multiwall carbon nanotubes) and of some of their elastomeric composites. *Vibrational Spectroscopy*. 2014;74:57-63. DOI:10.1016/j.vibspec.2014.07.009

29. Ferrari AC, Robertson J. Interpretation of Raman spectra of disordered and amorphous carbon. *Physical Review B*. 2000;61(20):14095-14107. DOI:10.1103/PhysRevB.61.14095

30. Pimenta MA, Dresselhaus G, Dresselhaus MS, Cançado LG, et al. Studying disorder in graphite-based systems by Raman spectroscopy. *Physical Chemistry Chemical Physics*. 2007;9(11):1276-1290. DOI:10.1039/B613962K

31. Ferrari AC, Rodil SE, Robertson J. Interpretation of infrared and Raman spectra of amorphous carbon nitrides. *Physical Review B*. 2003;67(15):155306. DOI:10.1103/PhysRevB.67.155306

32. Ferrari AC, Robertson J. Resonant Raman spectroscopy of disordered, amorphous, and diamondlike carbon. *Physical Review B*. 2001;64(7):075414. DOI:10.1103/PhysRevB.64.075414

33. Cançado LG, Jorio A, Ferreira EHM, Stavale F, et al. Quantifying defects in graphene via Raman spectroscopy at different excitation energies. *Nano Letters*. 2011;11(8):3190-3196. DOI:10.1021/nl201432g

34. Maslova OA, Ammar MR, Guimbretière G, Rouzaud JN, et al. Determination of crystallite size in polished graphitized carbon by Raman spectroscopy. *Physical Review B*. 2012;86(13):134205. DOI:10.1103/PhysRevB.86.134205

Information about the authors / Информация об авторах

Elena V. Kuzmina, Cand. Sc. (Chem.), Senior Scientist, Head of the Laboratory, Ufa Institute of Chemistry of Ufa Federal Research Centre of the Russian Academy of Sciences (UIC UFRS RAS), Ufa, Russian Federation, ORCID 0000-0002-3758-4762; e-mail: kuzmina@anrb.ru

Кузьмина Елена Владимировна, кандидат химических наук, старший научный сотрудник, заведующий лабораторией, Уфимский Институт химии Уфимского федерального исследовательского центра Российской академии наук (УФИХ УФИЦ РАН), Уфа, Российская Федерация; ORCID 0000-0002-3758-4762; e-mail: kuzmina@anrb.ru

Elvina R. Gaifullina, Laboratory Research Assistant, UIC UFRS RAS; Master's degree, Akmulla Bashkir State Pedagogical University, Ufa, Russian Federation; ORCID 0009-0005-3452-072X; e-mail: e.gaifullina02@mail.ru

Alena M. Ionina, Junior Scientist, PhD Student, UIC UFRS RAS, Ufa, Russian Federation; ORCID 0009-0005-4842-7294; e-mail: aionina27@xmail.ru

Elena V. Karaseva, Cand. Sc. (Chem.), Associate Professor, Leading Researcher, Head of Laboratory, UIC UFRS RAS, Ufa, Russian Federation; ORCID 0000-0002-8447-7230; e-mail: karaseva@anrb.ru

Vladimir S. Kolosnitsyn, D. Sc. (Chem.), Professor, Chief Scientist, Head of Department, UIC UFRS RAS, Ufa, Russian Federation; ORCID 0000-0003-1318-6943; e-mail: kolos@anrb.ru

Гайфуллина Эльвина Равилевна, лаборант-исследователь, УФИХ УФИЦ РАН; магистр, Башкирский государственный педагогический университет им. М. Акмуллы, Уфа, Российская Федерация; ORCID 0009-0005-3452-072X; e-mail: e.gaifullina02@mail.ru

Ионина Алена Михайловна, младший научный сотрудник, аспирант, УФИХ УФИЦ РАН, Уфа, Российская Федерация; ORCID 0009-0005-4842-7294; e-mail: aionina27@xmail.ru

Карасева Елена Владимировна, кандидат химических наук, доцент, ведущий научный сотрудник, заведующий лабораторией, УФИХ УФИЦ РАН, Уфа, Российская Федерация; ORCID 0000-0002-8447-7230; e-mail: karaseva@anrb.ru

Колосницын Владимир Сергеевич, доктор химических наук, профессор, главный научный сотрудник, заведующий отделом, УФИХ УФИЦ РАН, Уфа, Российская Федерация; ORCID 0000-0003-1318-6943; e-mail: kolos@anrb.ru

Received 12 August 2025; Revised 18 September 2025; Accepted 23 September 2025